Article:
Tafreshi, S.S., Taghizade, N., Sharifian, M. et al. (3 more authors) (Cover date: August 2023) A density functional theory study of CO2 hydrogenation on carbon-terminated TaC (111) surface. Reaction Kinetics, Mechanisms and Catalysis, 136. pp. 1945-1963. ISSN 1878-5190

https://doi.org/10.1007/s11144-023-02458-0

A Density functional theory study of CO_2 hydrogenation on carbon-terminated TaC (111) surface

Saeedeh Sarabadani Tafreshi[1, 2 *], Narges Taghizade[3], Mahmoodreza Sharifian[4], S. F. K. S. Panahi[3], Mostafa Torkashvand[1], Nora H. de Leeuw [2, 5]

[1]Department of Chemistry, Amirkabir University of Technology (Tehran Polytechnic), No. 350, Hafez Avenue, 1591634311 Tehran, Iran
[2]School of Chemistry, University of Leeds, LS2 9JT Leeds, UK
[3]Department of Physics, Iran University of Science and Technology, Narmak, 16846-13114 Tehran, Iran
[4]Department of Physics, North Tehran Branch, Islamic Azad University, 16511-53311 Tehran, Iran
[5]Department of Earth Sciences, Utrecht University, 3584 CB Utrecht, The Netherlands
*Correspondence: s.s.tafreshi@aut.ac.ir, S.SarabadaniTafreshi@leeds.ac.uk

Abstract

In this study, the density functional theory (DFT) implemented in the Vienna ab initio simulation package (VASP) was used to shed more light on the catalytic Carbon dioxide (CO_2) hydrogenation process on the (111) facet of the carbon-terminated tantalum carbide (TaC) surface. The adsorption of several intermediates and their hydrogenation elementary steps on the TaC (111) surface towards the formation and desorption of the main products including carbon monoxide (CO), methane (CH_4), and methanol (CH_3OH) was investigated. The results indicate that the involved intermediates adsorb strongly to the carbon-terminated TaC (111) surface by releasing large energies. The calculated reaction energies concluded in proposing the preferred mechanisms energetically, where the found pathways are overall endothermic which can be provided by the large exothermic adsorption energies of the intermediates. The favorite routes to the formation of desired compounds including CO, CH_4, and CH_3OH require overall reaction energies of 1.29, 5.96, and 6.63 eV, respectively, where they go through dihydroxycarbene (HOCOH) intermediate created from t-COOH hydrogenation. Along these routes, COH dehydrogenation to CO releases the largest exothermic reaction energy of -2.30 eV, while hydrogenation of t-HCOH to CH_2OH requires the highest endothermic reaction energy of 2.69 eV to proceed. It is concluded that CO and CH_4 are the main products of CO_2 hydrogenation on carbon terminated TaC (111) surface, in agreement with experimental and theoretical studies.

Keywords: Tantalum carbide, DFT, CO_2 hydrogenation, CH_4, CO, CH_3OH, TMC, TaC (111).

1. Introduction

Fossil fuel energy demand increased due to industrial growth, which has led to more pollution in the air as well as oceans. These pollutions have created greenhouse gasses along with ocean acidification, which are serious environmental concerns [1-4]. Specifically, the capturing and modification of CO_2 as a most blamed component, seems essential to stop more consequential damages in natural echo systems, meanwhile, obtaining valuable products could be hitting two birds with one stone.

Progressively, scientists are searching for negative emission technologies (NET) to reduce the emission of carbon dioxide through different strategies, such as biomass-based NET [5-8]. Alternatively, a crucial scene is the hydrogenation of CO_2 through utilizing novel catalysts to generate hydrocarbon products such as CO, HCOOH, CH_2O, CH_3OH, and CH_4 [9-15]. In the vicinity of an appropriate catalyst, the stable linear CO_2 molecule will be distorted by adsorption or chemisorption preparing to accept extra proton and electron as a result of changing anti-bonding energy states [9, 10, 16, 17].

Merging organic carbon atoms into a transition metal can lead to the formation of compounds called transitional metal carbides (TMCs) within the mixture properties of both ingredients such as firmness, high melting point, high corrosion resistance, and remarkable thermal and electrical conductivity due to the heritage in network solids, crystal lattice, and transition metal's properties [18-28].Remarkably, the presence of carbon could extremely change the catalytic properties of involved metals such as tungsten to platinum catalytic behavior as mentioned for the first time by Levy and Boudart in 1973 [29]. Besides, 2D TMCs structures known as MXenes are claimed to be the ambitious catalysts for some electro-catalytic reactions [30-32].

Recent experimental and DFT studies have shown that TMCs such as TiC, ZrC, WC, NbC, TaC, δ-MoC, β-Mo_2C, α-Mo_2C, WC, NbC, and NbC surfaces can be used for CO_2 activation [15, 28, 33-39] and conversion into CO [33, 40], CH_4 [13-15, 41], CH_3OH [34] and other compounds [42, 43]. Our previous DFT studies on TM and C-terminated NbC (111) and TM-terminated TaC (111) confirmed the catalytic activity of these surfaces towards CO_2 hydrogenations to CH_4 [13-15]. In the meantime, the interaction of hydrogen with the catalyst's surface has considerable importance

and it is accepted that the (111) orientation index sometimes is less stable and more active than the other low-index orientations [44, 45]. It was also found that CO_2 molecules were reduced more easily on the (111) facet of TiC and ZrC surfaces than on other facets [46, 47]. Generally, comprehensive studies have been done to explain the interaction between transition-metal carbide surface and hydrogen through angle-resolved photoemission technique showing preferred sites for adsorbing hydrogen [48-51]. The study by Aizawa et al. on hydrogen adsorption on IV and V TMC (111) surfaces by HREELS showed the vibrational frequency of hydrogen adsorption on TaC (111) surface at a much higher energy than those of other surfaces.[49] They attributed these observations to this fact that hydrogen is adsorbed on TaC (111) surface on a different site from the other TMC (111) surfaces and consistent with the formation of a CH species on the TaC (111) surface. They suggested that TaC (111) surface was carbon terminated, whereas other investigated surfaces were metal-terminated. Another study by Kitchin [52] also studies adsorption of hydrogen on C-terminated TMC (111) surfaces, where they found that H atom was stable only on TaC with high adsorption energy of -3.92 eV confirming that C–H species exist on the surface. It is also worth mentioning that TaC is stable to very high temperatures [53, 54]. According to the Quesne et al. study, the energy of the carbon and metal-terminated transition metal carbides (111) surfaces relaxations were calculated using DFT based on the difference in energy between the average cleavage values and the relaxed surface values which confirms that TaC demonstrate a preference for carbon-terminated (111) face [28].

Due to budgetary control in industrial production, an inexpensive hydrogen evolution reaction catalyst seems indispensable and triggers research on both theoretical and experimental domains. Based on the aforementioned motivation, this work committed to the theoretical evaluation that how a carbon termination surface of tantalum carbide (TaC) compound could be used as a catalyst for CO_2 conversion. In this regard, all possible pathways starting from adsorbed CO_2 until each final hydrocarbon stock has been tracked by calculating and comparing the energies of all possible intermediate steps.

Solving many-body Schrodinger equation is at the heart of quantum chemistry and it is critical to acquire a reasonable computational method. In contrast, to mean field wave function based Hartree-Fock and Post Hartree-Fock methods, the density functional theory (DFT) benefits from

spatial electronic density, proved to be quicker and more effective in this case, and will be used through this study as well as many studies in the literature [55-58].

2. Computational details

The plane-wave basis Viena Ab-initio Simulation Package (VASP) [59] was selected to establish density functional calculations, utilizing Perdew−Burke-Ernzerhof (PBE) [60] functional for the GGA approximation incorporated with London dispersion energy correction (DFT-D3) [61]. A plane wave cutoff energy of 600 eV was used for total energy calculations in both slab and bulk arrangements. Brillouin-zone integrations were performed using the 11×11×11 and 4×4×1 ***k***-point Monkhorst-Pack grid for bulk and surface, respectively. The calculated lattice constant of a_0 = 4.450 Å is in excellent agreement with experimental data (a_0 = 4.454 Å) [62] and the results of other DFT studies (a_0 = 4.485 and 4.436 Å) [23]. The periodic slab for the carbon-terminated TaC (111) surface is consisted of seven layers within 112 atoms where the top three layers were allowed to relax and four bottom layers are fixed to their bulk positions. A vacuum region of 20 Å was adopted to preclude interactions between slabs in the z-direction due to periodic nature of calculations. The self-consistent criteria in each iteration are 0.01 eV/Å and 10^{-5} eV for force tolerance and energy precision, respectively.

In this study we did not consider participation of surface carbon atoms in a way to have surface vacancies. We just considered the adsorption of the species on the carbon surface atoms, where each adsorbed intermediate is located in different initial positions on the surface including top, bridge, and hollow sites to calculate the favorable adsorption geometries. Based on this, the adsorption energy of each intermediate species (E_{ads}) was calculated by:

$$E_{ads} = E_{A+slab} - E_A - E_{slab}, \quad (1)$$

where E_{A+slab}, E_A, and E_{slab} denote the total energies of the relaxed adsorbates on the TaC (111) surface, the isolated adsorbates, and TaC (111) slab, respectively. Based on these definitions, the negative (positive) adsorption energy implies an exothermic (endothermic) process.

3. Results and discussion

3.1 Reaction networks of CO_2 hydrogenation

In the following sections, we provide a detailed investigation of the reaction network of all possible intermediates that are involved in the processes of CO_2 hydrogenation on C-terminated TaC (111) surfaces. To end this, we first optimized all of the intermediates on the C-terminated TaC (111) surface to explore the most favorable adsorption site and geometry which will have been explained in detail in the next section. Various particular elementary steps for the reaction map of CO_2 hydrogenation to CO, HCOOH, CH_2O, CH_3OH, and CH_4 on the C-terminated TaC (111) surface are demonstrated in Figure 1. Initially, the main trend of the reaction network includes pathways either from HCOO or from (c,t)-COOH.

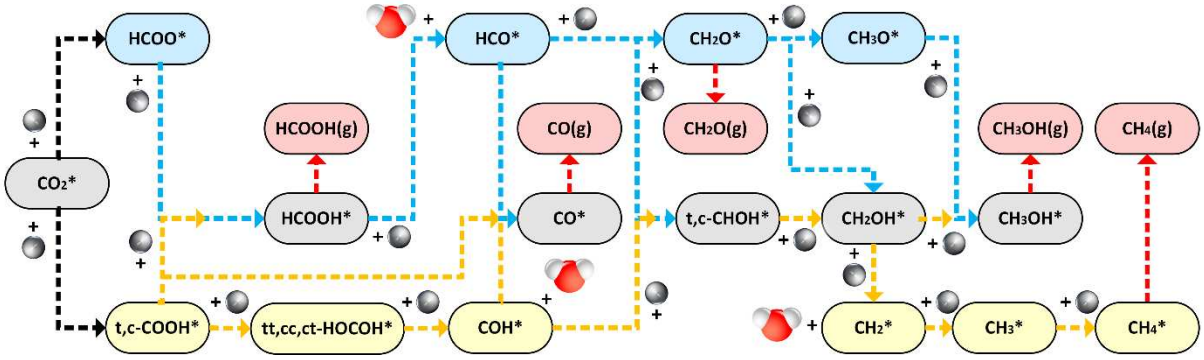

Figure 1. The possible reaction networks of CO_2 hydrogenation to CO, HCOOH, CH_2O, CH_3OH, and CH_4 on the TaC (111) surface.

3.2 Adsorption configurations and energies on TaC (111) surface

To map the most efficient and probable reaction path of CO_2 hydrogenation on C-terminated TaC (111) surface, we have optimized all involved intermediates, searching for the most favorable sites as well as molecules' relaxed structures and related energies through starting from several initial configurations (see Figure. 2 and Table 1). The results of our previous study of the adsorption energies of intermediates on Ta-terminated TaC (111) are also reported in Table 1 to be able to compare the effect of surface termination on the intermediates' adsorption energies.

The carbon atom tends to relax on the C atom of the TaC (111) surface forming a strong bond with adsorption energy -11.3 eV and a C–C bond length equal to 1.35 Å. Besides, the hydrogen atom finds its best position right above the C atom of the TaC (111) surface forming an H–C bond with a length of 1.098 Å. Both H_2O and OH rest in the bridge position near the C atoms of TaC (111)

surface while the OH position is more perfect in which the oxygen atom bonds to the carbon atom with energy -4.93 eV and adsorption energy of H_2O is -1.32 eV. CH prefers to adsorb nearly on top of the C atom of the TaC (111) surface with bond length and adsorption energy of 1.28 Å and -9.13 eV, respectively. CO binds to TaC (111) surface through its C atom which is located exactly at top of the carbon atom of the surface with a C–C bond length of 1.32 Å and an adsorption energy of -3.93 eV.

The results show that the CO_2 molecule can't form any chemical bond to TaC (111) surface within the least deformation in CO_2 structure and bond length, such that the C–O bond length and C–O–C angle are 1.177 Å and 179.58° which indicate slight variation relative to free CO_2 geometric parameters (1.177 Å and 180°), respectively (see Figure 2-a, b).

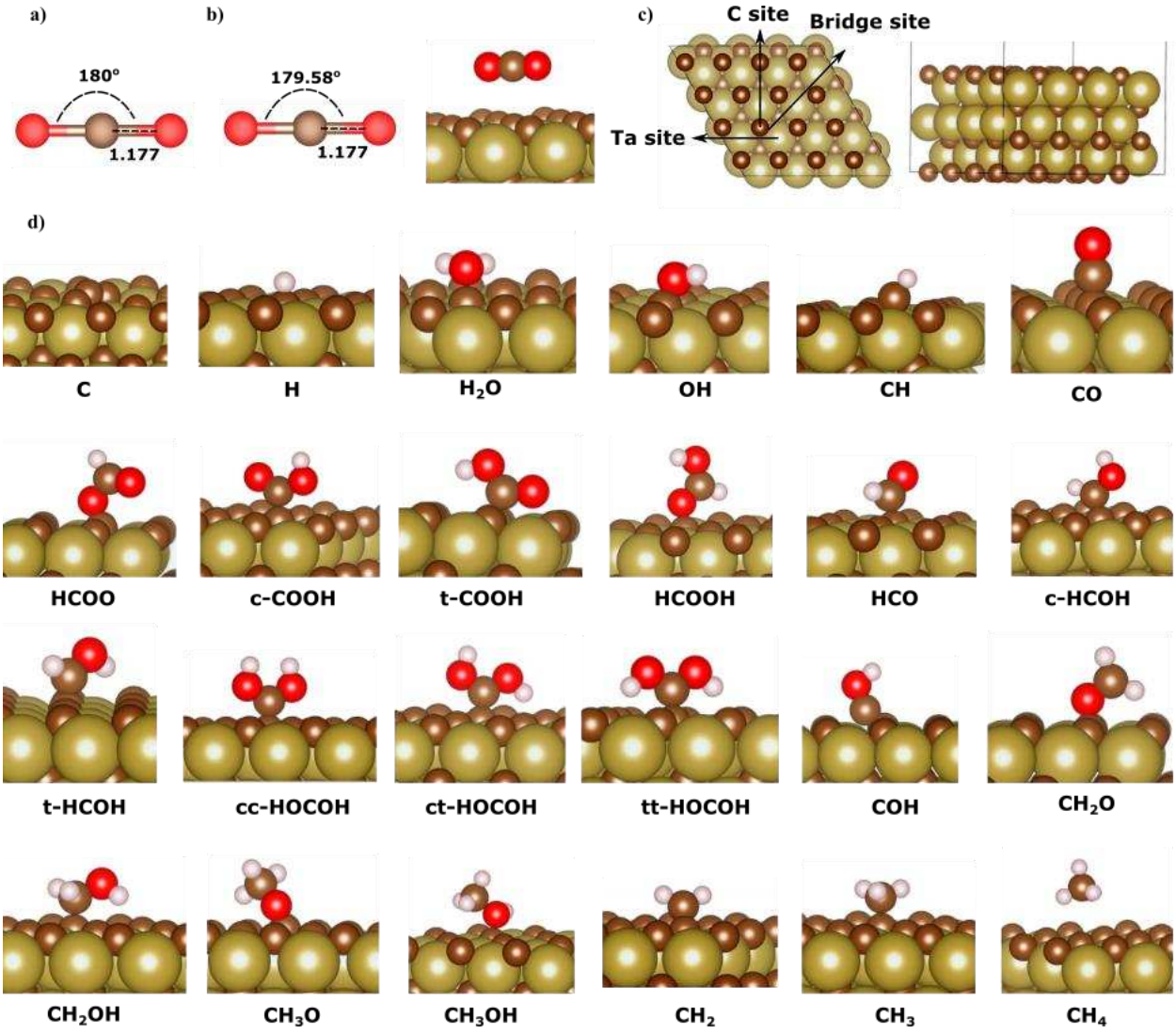

Figure 2. The isolated CO_2 molecule, a) before, and b) after adsorption, c) TaC (111) surface and d) adsorption geometries of the involved structures in CO_2 hydrogenation on TaC (111) surface.

The connection bond between HCOO and TaC (111) surface occurs through C–O bond with a length of 1.31 Å and an adsorption energy of -3.48 eV. Both cis and trans configurations of COOH got connected to the TaC surface via their C atom and have C–C bonds with lengths of 1.49 and 1.41 Å, respectively. The c-COOH relaxes right on top of the C atom, meanwhile, t-COOH tends toward the bridge position and its O atom makes a bond with Ta. The adsorption energies of c-COOH and t-COOH are -4.11 eV and -4.13 eV, respectively. In HCOOH, the molecule prefers to be adsorbed via its O atom forming an O–C bond with a length of 1.42 Å and an adsorption energy of -1.53 eV. Meanwhile, the process alters the lengths of two C–O bonds of HCOOH about a 5% decrease in closer bond to the surface and a 7% rise in farther bond from the surface. HCO binds

to the surface through its carbon on the top of the C atom of TaC forming a C–C bond equal to 1.05 Å within adsorption energy -4.168. In a similar fashion, the carbon atom of c-HCOH and t-HCOH make bonds with the C atom of TaC (111) surface with C–C bond lengths of 1.38 and 1.39 Å, respectively. However, the optimized positions are different such that the t-HCOH locates right above the C atom of the surface with an adsorption energy of -4.806 while c-HCOH tends toward a bridge position with energy equal to -6.18 eV. The HCOCH molecule adsorbs in three different configurations, namely, cc-HOCOH, ct-HOCOH, and tt-HOCOH all making C–C bonds with lengths of 1.38, 141 and 1.42 Å and adsorption energies -4.806, -5.321, and -5.60 eV, respectively. Both COH and CH_2O adsorb on the C atom of the TaC surface releasing energies corresponding to -6.83 and -1.84 eV, respectively. Furthermore, COH connects to the TaC surface through its C atom forming a C–C bond (1.29 Å), although CH_2O prefers to make a C–O bond (1.38 Å).

Table 1. The adsorption energies (E_{ads}) and geometric details of the preferred adsorbed structures of all intermediates during CO_2 hydrogenation on carbon-terminated TaC (111) surface. The adsorption energies (E_{ads}) of the intermediates on Ta-terminated TaC (111) are also reported for comparison[13]. Star symbol (*) indicates the existing bond between the intermediate and surface, while there is no symbol for the bonds inside each intermediate during its adsorption on the catalyst surface.

Species	E_{ads} (eV) on C-terminated TaC (111)	E_{ads} (eV) on Ta-terminated TaC (111) [13]	Bond length (Å)	Species	E_{ads} (eV) on C-terminated TaC (111)	E_{ads} (eV) on Ta-terminated TaC (111) [13]	Bond length (Å)
H	-5.15, -3.92[52], -5.130[14], -3.52[63]	–	d^*_{H-C} = 1.09	t-HCOH	-6.31, -6.342[14], -5.35[63]	–	d^*_{C-C} = 1.39, d_{O-C} = 1.31
C	-11.40, -11.757[14], -7.61[63]	–	d^*_{C-C} = 1.36	cc-HOCOH	-4.81, -4.824[14]	-0.59	d^*_{C-C} = 1.39, d_{O-C} = 1.33
H_2O	-1.23, -0.997[15], -1.33[64], -1.226[14]	–	d^*_{O-C} = 1.51, d_{H-O} = 1.00	ct-HOCOH	-5.32, -5.302[14]	-0.74	d^*_{C-C} = 1.41, d_{O-C} = 1.32
OH	-4.93, -5.304[14], -5.52[63], -5.427[15]	–	d^*_{C-O} = 1.31, d_{H-O} = 0.99	tt-HOCOH	-5.60, -5.561[14]	-0.85	d^*_{C-C} = 1.42, d_{O-C} = 1.31
CH	-9.13, -9.442[14], -7.29[63], -7.404[15]	–	d^*_{C-C} = 1.28,	COH	-6.83, -7.347[14], -4.88[63]	-0.23	d^*_{C-C} = 1.29, d_{O-C} = 1.28
CO	-3.93, -4.008[14], -2.48[63]	-0.23	d^*_{C-C} = 1.32, d_{O-C} = 1.16	CH_2O	-1.84, -1.908[14] -2.63[63]	-0.33	d^*_{O-C} = 1.38, d_{O-C} = 1.28
CO_2	-0.13, -0.358[14], -0.27[64]	-1.90	d_{C-O} = 1.177	CH_2OH	-4.23, -4.219[14], -3.293[15],	-0.75	d^*_{C-C} = 1.51, d_{O-C} = 1.40

					-3.09[63]		
HCOO	-3.48, -5.222[15]	-0.48	d^*_{C-O} = 1.31	CH_3O	-6.06, -4.52[63]	-0.64	d^*_{O-C} = 1.28
c-COOH	-4.11, -4.155[14], -4.105[15]	-0.62	d^*_{C-C} = 1.49, d_{O-C} = 1.22, d_{O-C} = 1.36	CH_3OH	-1.68, -1.614[14], -0.72[63], -0.959[15]	-0.14	d^*_{O-C} = 1.47
t-COOH	-4.13, -4.408[14], -3.959[15]	-0.70	d^*_{C-C} = 1.41, d^*_{O-Ta} = 2.39, d_{O-C} = 1.27, d_{O-C} = 1.32	CH_2	-7.32, -7.418[14], -5.797[15], -5.81[63]	-0.61	d^*_{C-C} = 1.37
HCOOH	-1.53, -1.539[14], -1.642[15]	-0.71	d^*_{C-O} = 1.42, d_{O-C} = 1.28, d_{O-C} = 1.30	CH_3	-4.50, -4.528[14], -3.58[63], -3.721[15]	-1.00	d^*_{C-C} = 1.50, d_{H-C} = 1.10
HCO	-4.17, -4.214[14], -3.74[63], -4.240[15]	-0.33	d^*_{C-C} = 1.50, d_{O-C} = 1.22	CH_4	-0.11 -0.161[14], -0.298[15], -0.17[63]	-0.09	d_{H-C} = 1.10
c-HCOH	-6.18, -6.232[14]	-0.46	d^*_{C-C} = 1.38, d_{O-C} = 1.33				

CH_2OH rests on the C atom of the TaC surface with an adsorption energy of -4.23 eV and a C–C bond length of 1.51 Å. However, CH_3O makes a O–C bond with a length of 1.28 Å by releasing an adsorption energy of 6.06 eV. The oxygen atom in CH_3OH tends to make an O–C bond with a TaC surface equal to 1.47 Å where the adsorption energy is -1.68 eV. The carbon atom in both CH_2 and CH_3 make a C–C bond on the TaC surface while in CH_3 the carbon is perfectly above the C site of the TaC (111) surface. Here, the bond lengths are 1.37 and 1.50 Å, and the corresponding adsorption energies are -7.32 and -4.50 eV, respectively. The methane molecule (CH_4) hovers on the TaC surface with a minimum distance for its carbon of about 2.81 Å with a low adsorption energy of -0.11 eV.

The results of this section indicate that the studied intermediates of CO_2 hydrogenation on C-terminated TaC (111) surface adsorb via their carbon atoms to the surface carbon atoms strongly by releasing large energies. As Table 1 shows these findings are in agreement with the studies where these intermediates adsorb on the Mo_2C and NbC surfaces strongly by the formation of C–C bonds [14, 63]. Table 1 also confirms that intermediates adsorb stronger on the C-terminated TaC (111) surface than Ta-terminated TaC (111) surface.

3.3 Chemical Reactions

In the previous section, we explained the stable geometries of all intermediates involved in the reaction networks. To follow our investigation, the reaction energies of all intermediates'

hydrogenations on C-terminated TaC (111) surface are presented in Table 2. The results of our previous study of the reaction energies on Ta-terminated TaC (111) are also reported in Table 2 to be able to compare the effect of surface termination on the intermediates' reaction energies.

The initial step of CO_2 hydrogenation is either the formation of the formate ($HCOO^*$) via $CO_2^* + H^* \rightarrow HCOO^*$ or the carboxyl species (t-$COOH^*$ and/or c-$COOH^*$) through $CO_2^* + H^* \rightarrow$ (c,t)-$COOH^*$ reaction formula. The former is characterized as an endothermic process with 1.11 eV and the latter contains the formation of t-$COOH^*$ with endothermic energy of 0.06 eV and c-$COOH^*$ which is also an endothermic reaction with 0.20 eV energy. Further hydrogenation of $HCOO^*$ brings about the formation of formic acid (HCOOH) through $HCOO^* + H^* \rightarrow HCOOH^*$ reaction formula with an endothermic energy of 0.96 eV. $HCOOH^*$ could also be produced from carboxyl species where, c-$COOH^*$ and t-$COOH^*$ react with H via c,t-$COOH^* + H^* \rightarrow HCOOH^*$ reactions. Both reactions are characterized as an endothermic process with corresponding energy of 1.87 and 2.01 eV for cis and trans conformers, respectively. From reaction energies, it is clear that the formation of $HCOOH^*$ via formate is more feasible than that of c,t-$COOH^*$ intermediates. Subsequent hydrogenation of c-COOH and t-COOH lead to the generation of dihydroxycarbene species (cc-$HOCOH^*$, ct-$HOCOH^*$, and tt-$HOCOH^*$). In which, the formation of tt-$HOCOH^*$ (t-$COOH^* + H^* \rightarrow$ tt-$HOCOH^*$) and ct-$HOCOH^*$ (c-$COOH^* + H^* \rightarrow$ ct-$HOCOH^*$) are exothermic processes with energies of -0.22 and -0.08 eV, while t-$COOH^* + H^* \rightarrow$ ct-$HOCOH^*$ reaction is endothermic with corresponding energy of 0.06 eV. Moreover, the calculated energies show that the transformation of (cc,ct)-$HOCOH^*$ to tt-$HOCOH^*$ is exothermic with reaction energies of -1.03 eV and -0.28 eV for cc-$HOCOH^*$ and ct-$HOCOH^*$ species, respectively. As a result, there are two paths including either from $HCOOH^*$ or from $HOCOH^*$ intermediate which one can follow for CO_2 hydrogenation to HCOOH, CO, CH_2O, CH_3OH, and CH_4 on the TaC (111) surface. In the following, these reaction paths have been presented in detail, and also, the reaction profiles and corresponding energy values of different routes for CO_2 hydrogenation of intermediates are depicted in Figure 3.

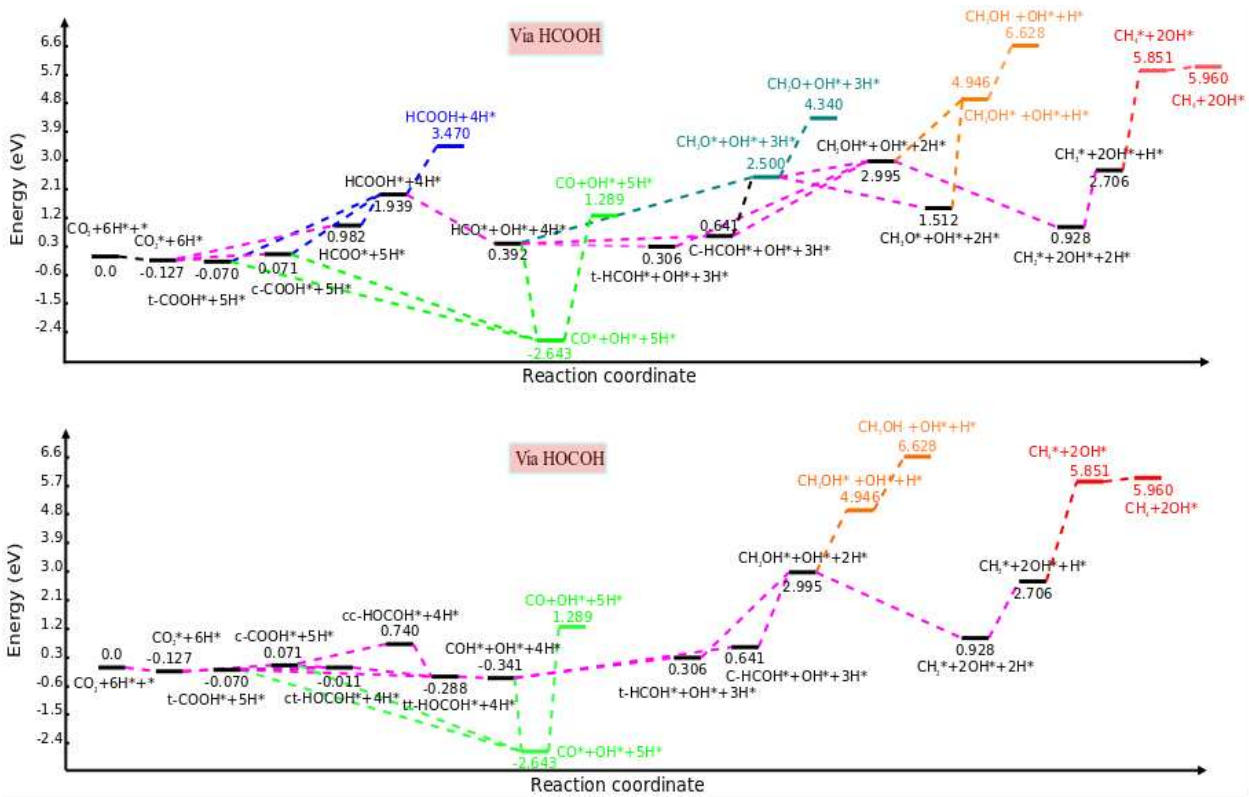

Figure 3. Reaction profile for CO_2 and subsequent hydrogenation of intermediates to HCOOH, CO, CH_2O, CH_3OH, and CH_4 via a) HCOOH and b) HOCOH on the TaC (111) surface.

Table 2. The possible reactions and their corresponding energies (ΔE) in the hydrogenation of intermediates to form CO, HCOOH, CH_2O, CH_3OH and CH_4. The reaction energies (ΔE) of the intermediate's hydrogenations on Ta-terminated TaC (111) are also reported for comparison [13].

Elementary Reactions	**ΔE(eV)** on C-terminated TaC (111)	**ΔE(eV)** on Ta-terminated TaC (111) [13]	**Elementary Reactions**	**ΔE(eV)** on C-terminated TaC (111)	**ΔE(eV)** on Ta-terminated TaC (111) [13]
$CO_2(g) \rightarrow CO_2^*$	-0.13	-1.89	$c\text{-}COOH^* + H^* \rightarrow cc\text{-}HOCOH^*$	0.67	1.84
$CO_2^* + H^* \rightarrow HCOO^*$	1.113	0.20	$t\text{-}COOH^* + H^* \rightarrow tt\text{-}HOCOH^*$	-0.22	1.67
$CO_2^* + H^* \rightarrow c\text{-}COOH^*$	0.20	1.06	$c\text{-}COOH^* + H^* \rightarrow ct\text{-}HOCOH^*$	-0.08	1.70
$CO_2^* + H^* \rightarrow t\text{-}COOH^*$	0.06	0.97	$t\text{-}COOH^* + H^* \rightarrow ct\text{-}HOCOH^*$	0.06	1.78
$c\text{-}COOH^* \rightarrow t\text{-}COOH^*$	-0.14	-0.08	$cc\text{-}HOCOH^* + H^* \rightarrow tt\text{-}HOCOH^*$	-1.03	-0.26
$HCOO^*+H^* \rightarrow HCOOH^*$	0.96	1.58	$ct\text{-}HOCOH^* + H^* \rightarrow tt\text{-}HOCOH^*$	-0.28	-0.11

c-$COOH^*$ → CO^* + OH^*	-2.71	0.70	tt-$HOCOH^*$ → COH^* + OH^*	-0.05	-1.38
t-$COOH^*$ → CO^* + OH^*	-2.57	0.78	ct-$HOCOH^*$ → COH^* + OH^*	-0.33	-1.49
c-$COOH^*$ + H^* → $HCOOH^*$	1.87	0.72	cc-$HOCOH^*$ → COH^* + OH^*	-1.08	-1.64
t-$COOH^*$ + H^* → $HCOOH^*$	2.01	0.80	COH^* → CO^* + H^*	-2.30	0.49
$HCOOH^*$ → HCO^* + OH^*	-1.55	-1.61	COH^* + H^* → t-$HCOH^*$	0.65	–
$HCOOH^*$ → HCOOH(g)	1.53	2.32	COH^* + H^* → c-$HCOH^*$	0.98	0.59
HCO^* + H^* → t-$HCOH^*$	-0.09	–	t-$HCOH^*$ + H^* → CH_2OH^*	2.69	–
HCO^* + H^* → c-$HCOH^*$	0.25	1.69	c-$HCOH^*$ + H^* → CH_2OH^*	2.35	0.52
HCO^* → CO^* + H^*	-3.04	1.59	CH_2OH^* + H^*→ CH_3OH^*	1.95	1.42
CO^* → CO(g)	3.93	0.26	CH_2OH^* → CH_2^* + OH^*	-2.07	-1.85
HCO^* + H^* → CH_2O^*	2.11	0.81	CH_2^* + H^* → CH_3^*	1.78	0.43
CH_2O^* → CH_2O(g)	1.84	2.83	CH_3^* + H^* → CH_4^*	3.14	1.82
CH_2O^* + H^* → CH_3O^*	-0.99	0.50	CH_4^* → CH_4(g)	0.11	0.24
CH_2O^* + H^* → CH_2OH^*	0.50	1.40	CH_3OH^* → CH_3OH(g)	1.68	1.04
CH_3O^* + H^* → CH_3OH^*	3.43	2.32	H_2O^* → H_2O(g)	1.23	0.90

3.3.1 Reaction Pathways of CO_2 to possible products through HCOOH

3.3.1.1 The reaction paths for the CO_2 hydrogenation to HCOOH

As discussed above, hydrogenation of CO_2 can result in either formation of $HCOO^*$ or t-$COOH^*$ and/or c-$COOH^*$. Subsequent hydrogenation of these species yields an HCOOH product. Therefore, there are three available paths one can follow to achieve HCOOH, a path through $HCOO^*$ where, $HCOO^*$ obtains another hydrogen and forms $HCOOH^*$. The other two paths contain the routes from t-$COOH^*$ or c-$COOH^*$ species. In the former, t-$COOH^*$ take hydrogen and make $HCOOH^*$ with endothermic energy of 2.01 eV and the latter takes place through c,t-$COOH^*$ + H^* → $HCOOH^*$ with 1.87 eV energy. Bearing in mind $HCOOH^*$ → HCOOH (g) reaction, leading to HCOOH (g) is an endothermic process that requires 1.53 eV energy, indicating that $HCOOH^*$ may not prefer to be desorbed from the surface.

3.3.1.2 The reaction paths for the CO_2 hydrogenation to CO via HCOOH

Decomposition of (t,c)-$COOH^*$ via reaction formula of (c,t)-$COOH^* \rightarrow CO^* + OH^*$ result in the production of CO which are exothermic reactions with energies of -2.71 and -2.57 eV for cis and trans conformers, respectively. On the other side, $HCOOH^*$

A way to get CH_2O includes only a path through HCO^*, where, HCO^* can accept hydrogen and form CH_2O^*. From Table 2, this reaction is endothermic and requires 2.11 eV energy to proceed. Similar to $HCOOH^*$, producing CH_2O ($CH_2O^* \rightarrow CH_2O$ (g)) is an endothermic process with 1.84 eV energy indicating that the desorption of CH_2O^* from the surface may not thermodynamically possible.

3.3.1.4 The reaction paths for the CO_2 hydrogenation to CH_3OH via HCOOH

Besides CH_2O^*, the hydrogenation of HCO^* throughout $HCO^* + H^* \rightarrow$ (c,t)-$HCOH^*$ reaction, yields the formation of (c,t)-$HCOH^*$ with energies of -0.09 and 0.25 eV for trans and sis formations, respectively. It seems t-$HCOH^*$ is the preferred conformer due to its exothermic reaction. Then (c,t)-$HCOH^*$ further reacts with hydrogen to form CH_2OH^* and both reactions are distinguished as endothermic processes with energies of 2.69 and 2.35 eV within related t-$HCOH^* + H^* \rightarrow CH_2OH^*$ and c-$HCOH^* + H^* \rightarrow CH_2OH^*$ reactions, respectively. Subsequent hydrogenation of produced CH_2OH^* appears to make CH_3OH^* via $CH_2OH^* + H^* \rightarrow CH_3OH^*$, which is also an endothermic reaction with an energy of 1.95 eV. Therefore, The path to get CH_3OH contains a way through either (c,t)-$HCOH^*$ or CH_2O^* which the former are explained above. However, the latter reaction includes hydrogenation of formaldehyde intermediate where CH_2O^* takes hydrogen to make either CH_2OH^* or CH_3O^*. Reaction $CH_2O^* + H^* \rightarrow CH_2OH^*$ is endothermic and requires 0.49 eV energy. Also, $CH_2O^* + H^* \rightarrow CH_3O^*$ could be known as an exothermic process with -0.99 eV. Additional hydrogenation of CH_2OH^* or CH_3O^* can create CH_3OH^*. Based on this, CH_3OH^* may be produced via $CH_2OH^* + H^* \rightarrow CH_3OH^*$ with the reaction energy of 1.95 eV or from $CH_3O^* + H^* \rightarrow CH_3OH^*$ with the reaction energy of 3.43 eV. Since this process energetically is not feasible, one could conclude that the pathway to CH_3OH^* product follows from CH_2OH^* hydrogenation path rather than CH_3O^* one. As $CH_3OH^* \rightarrow CH_3OH$ (g) is endothermic with 1.68 eV energy. Then, the desorption of CH_3OH^* from the surface is not expected.

3.3.1.5 The reaction paths for the CO_2 hydrogenation to CH_4 via HCOOH

The route for CH_4^* formation involves the dissociation of CH_2OH^* via $CH_2OH^* \rightarrow CH_2^* + OH^*$ releasing the energy of -2.07 eV leading to CH_2^* formation. Afterwards, successive hydrogenations of CH_2^* and CH_3^* produce CH_3^* and CH_4^* through reactions of $CH_2^* + H^* \rightarrow CH_3^*$ and $CH_3^* + H^* \rightarrow CH_4^*$ with energies of 1.78 and 3.14 eV, respectively.

3.3.2 Reaction Pathways of CO_2 to possible products through HOCOH

As mentioned before, there are two paths to reach CO, CH_3OH, and other final products. In these following sections, we consider a route through $HOCOH_*$ intermediates, where $HOCOH^*$ is produced by hydrogenation of c,t-$COOH^*$ via (c,t)-$COOH^* + H^* \rightarrow$ (ct, cc, tt)-$HOCOH^*$. Comparing the conversion energies of cc- $HOCOH^*$ to tt- $HOCOH^*$ (cc-$HOCOH^* \rightarrow$ tt-$HOCOH^*$) (-0.28 eV) and ct- $HOCOH^*$ to tt- $HOCOH^*$ (ct-$HOCOH^* \rightarrow$ tt-$HOCOH^*$) (-1.08 eV), offers that the tt-$HOCOH^*$ is preferable conformer. Therefore, the path to get possible products more likely involves the tt-$HOCOH^*$ intermediate.

3.3.200000000.1 The reaction paths for the CO_2 hydrogenation to CO via HOCOH

There are two paths for carbon mono oxide (CO) termination. The first route starts from (c,t)-$COOH^*$ intermediates and continues via (c,t)-$COOH^* \rightarrow CO^* + OH^*$ reaction by releasing exothermic energies of -2.71 and -2.57 eV for cis and trans configurations, respectively. The second way is disintegrating of $HOCOH^*$ conformers through (tt, ct, cc)-$HOCOH^* \rightarrow COH^* + OH^*$ reactions with energies of -0.05, -0.33, and -1.08 eV, correspondingly. Finally, further decomposition of COH^* via ($COH^* \rightarrow CO^* + H^*$) within -2.30 eV energy leads to the production of CO^*. As all the above-mentioned reactions are exothermic, CO^* may be produced via all of these routes.

3.3.2.2 The reaction paths for the CO_2 hydrogenation to CH_3OH via HOCOH

Here, we start from the hydrogenation of COH^* tracking the chemical path that ends up on CH_3OH. Mentioned hydrogenation leads to trans-$HCOH^*$ and cis-$HCOH^*$ configurations through $COH^* + H^* \rightarrow$ t-$HCOH^*$ and $COH^* + H^* \rightarrow$ c-$HCOH^*$ with endothermic energies of 0.65 and 0.98 eV, respectively. Once $HCOH^*$ conformers get another hydrogen, CH_2OH^* is produced through (t,c)-$HCOH^* + H^* \rightarrow CH_2OH^*$ reactions, where both are endothermic processes with 2.69 and 2.35 eV

for t-HCOH* and c-HCOH* conformers, respectively. Finally, further hydrogenation of CH_2OH^* leads to the production of CH_3OH^*. This reaction takes place via $CH_2OH^* + H^* \rightarrow CH_3OH^*$ with 1.95 eV energy.

3.3.2.3 The reaction paths for the CO_2 hydrogenation to CH_4 via HOCOH

The path that reaching CH_4^* production, contains the dissociation of CH_2OH^* generating CH_2^* intermediate ($CH_2OH^* \rightarrow CH_2^* + OH^*$). This reaction seems feasible as characterized as an exothermic process with -2.07 eV negative energy. Over the succeeding hydrogenations of CH_2^* and CH_3^*, CH_4^* will be produced via $CH_2^* + H^* \rightarrow CH_3^*$ and $CH_3^* + H^* \rightarrow CH_4^*$ reactions with 1.78 and 3.14 eV reaction energies, respectively.

Conclusion

In this study, the energetics of the reaction networks of CO_2 hydrogenation on the C-terminated TaC (111) surface were investigated. We have calculated the reaction energies of the elementary steps of several intermediates' hydrogenations towards the formation of CH_2O, HCOOH, CO, CH_4, and CH_3OH as products. From the energetic results in the previous sections, we can conclude the preferred mechanisms leading to the predominant products from the studied compounds in this work.

The investigated pathways in this study are considered to go through HCOOH or HOCOH. According to our findings, the hydrogenation pathway via HOCOH is more favored energetically and is more likely to happen. As it is clear from Figure 3, the preferred hydrogenation route starting from CO_2 and ending to tt-HOCOH is less endothermic than the one ending with HCOOH, where both go via t-COOH:

$$CO_2(g) \xrightarrow{\Delta E=-0.127} CO_2^* \xrightarrow{\Delta E=0.057} \text{t-COOH}^* \xrightarrow{\Delta E=-0.218} \text{tt-HOCOH}^* \quad (2)$$

$$CO_2\,(g) \xrightarrow{\Delta E=-0.127} CO_2^* \xrightarrow{\Delta E=0.057} \text{t-COOH}^* \xrightarrow{\Delta E=2.010} \text{HCOOH}^* \quad (3)$$

Therefore, the suggested pathway for all products starts with the reaction (1). Since according to Figure 3, all the routes over C-terminated TaC (111) are endothermic mechanisms for product generation, we choose the less endothermic routes as the energetic-preferred pathway for each possible product. The pathway with total endothermic energy of 1.29 eV is the least endothermic

CO_2 hydrogenation mechanism to CO as the first possible product:

$$CO_2\ (g) \xrightarrow{\Delta E=-0.127} CO_2{}^* \xrightarrow{\Delta E=0.057} \text{t-COOH}^* \xrightarrow{\Delta E=-0.218} \text{tt-HOCOH}^* \xrightarrow{\Delta E=-0.053}$$

$$COH^* \xrightarrow{\Delta E=-2.302} CO^* \xrightarrow{\Delta E=3.932} CO\ (g) \quad (4)$$

CH_4 is the second product of CO_2 hydrogenation over C-terminated TaC (111) surface that needs the total endothermic reaction energy of 5.96 eV to be formed and released from the surface (Figure 3) with the preferred route:

$$CO_2\ (g) \xrightarrow{\Delta E=-0.127} CO_2{}^* \xrightarrow{\Delta E=0.057} \text{t-COOH}^* \xrightarrow{\Delta E=-0.218} \text{tt-HOCOH}^* \xrightarrow{\Delta E=-0.053}$$

$$COH^* \xrightarrow{\Delta E=0.647} \text{t-HCOH}^* \xrightarrow{\Delta E=2.689} CH_2OH^* \xrightarrow{\Delta E=-2.067} CH_2{}^* \xrightarrow{\Delta E=1.778}$$

$$CH_3{}^* \xrightarrow{\Delta E=3.145} CH_4{}^* \xrightarrow{\Delta E=0.108} CH_4\ (g) \quad (5)$$

The third mechanism, needing energy of 6.63 eV, results in CH_3OH formation, shown in Figure 3:

$$CO_2\ (g) \xrightarrow{\Delta E=-0.127} CO_2{}^* \xrightarrow{\Delta E=0.057} \text{t-COOH}^* \xrightarrow{\Delta E=-0.218} \text{tt-HOCOH}^* \xrightarrow{\Delta E=-0.053}$$

$$COH^* \xrightarrow{\Delta E=0.647} \text{t-HCOH}^* \xrightarrow{\Delta E=2.689} CH_2OH^* \xrightarrow{\Delta E=1.952} CH_3OH^* \xrightarrow{\Delta E=1.682} CH_3OH\ (g) \quad (6)$$

From the above, we can see that CO, CH_4, and CH_3OH productions are endothermic with total reaction energies of 1.29, 5.96, and 6.63 eV on C-terminated TaC (111), whereas according to our previous study of CO_2 hydrogenation reactions on Ta-terminated TaC (111) surface [13], formation of CO, CH_4, and CH_3OH are exothermic with releasing energies of 2.55, 4.24, 2.10 eV. Even though the overall reaction energies for the preferred mechanisms on C-terminated TaC (111) compared to those on Ta-terminated TaC (111) are highly endothermic for CO, CH_4, and CH_3OH productions, the release of the calculated adsorption energies of the involved species on the surface is large enough to provide sufficient energy for the endothermic hydrogenation reactions and desorption energies needed for the products to get away from the catalyst surface. It is concluded that CO and CH_4 as the main and abundant products of CO_2 hydrogenation on the both C and Ta-terminated TaC (111) surfaces, inconsistent with experimental and theoretical studies of CO_2 hydrogenation on transition metal carbides [14, 15, 40, 63, 65].

From these results, we can see that the main products of CO and CH_4 are produced via the tt-HOCOH route, where the highest exothermic energy of -2.30 eV and endothermic reaction energy of 2.69 eV belong to the dehydrogenation of COH^* to CO^* and hydrogenation of t-$HCOH^*$ to CH_2OH^*, respectively.

The adsorption energies of the intermediates on the surface exhibit intense, localized, and robust interactions between the adsorbates and the surface. These interactions create an overall exothermic reaction pathway, generating ample energy to surpass the desorption energy required for releasing the products from the surface. Moreover, when hydrogen and the intermediates are co-adsorbed on the surface, the hydrogenation step energies suggest that the presence of hydrogen enhances the reactivity of the intermediates. Consequently, the intermediates readily engage in additional surface-mediated reactions, leading to the formation of CO, CH_4, and other products.

It is worth mentioning that this research solely focused on examining the thermodynamics of the reactions while neglecting the kinetics and activation energies. The suggested mechanisms were derived from a comparison of reaction energies among various pathways, revealing the energetically preferred reaction mechanism. Although the incorporation of transition states in catalytic pathways would offer additional insights, such as identifying the rate-determining step, it would not negate the thermodynamically favorable reaction pathway.

This study's findings assist in understanding the energetics of some elementary reactions in CO_2 hydrogenation on C-terminated TaC (111) surfaces and the development of transition metal carbides as effective experimental catalysts in the field of CO_2 hydrogenation. There is still a need to investigate CO_2 hydrogenation mechanisms towards other hydrocarbon productions.

Data Availability Statement: The data that support the findings of this study are available from the corresponding author upon reasonable request.

Acknowledgments: S.S.T thanks the Iran National Science Foundation (INSF) Grant No. 97020912 for the financial support of this investigation. The authors are also grateful to the Research Affairs Division of the Amirkabir University of Technology (AUT), Tehran, Iran, for their financial support.

Conflicts of Interest: There are no competing interest to declare.

References

1. Houghton J (2005) Global warming. Reports on Progress in Physics 68(6):1343-403. 10.1088/0034-4885/68/6/r02.
2. Kaplan JO, New M (2006) Arctic climate change with a 2 ◦C global warming: Timing, climate patterns and vegetation change. Climatic Change 79(3):213-41. 10.1007/s10584-006-9113-7.
3. Kellstedt PM, Zahran S, Vedlitz A (2008) Personal Efficacy, the Information Environment, and Attitudes Toward Global Warming and Climate Change in the United States. Risk Analysis 28(1):113-26. https://doi.org/10.1111/j.1539-6924.2008.01010.x.
4. Liverman DM, O'Brien KL (1991) Global warming and climate change in Mexico. Global Environmental Change 1(5):351-64. https://doi.org/10.1016/0959-3780(91)90002-B.
5. McLaren D (2012) A comparative global assessment of potential negative emissions technologies. Process Safety and Environmental Protection 90(6):489-500. https://doi.org/10.1016/j.psep.2012.10.005.
6. Haszeldine RS, Flude S, Johnson G, Scott V (2018) Negative emissions technologies and carbon capture and storage to achieve the Paris Agreement commitments. Philosophical Transactions of the Royal Society A: Mathematical, Physical and Engineering Sciences 376(2119):20160447. doi:10.1098/rsta.2016.0447.
7. Bednar J, Obersteiner M, Wagner F (2019) On the financial viability of negative emissions. Nature Communications 10(1):1783. 10.1038/s41467-019-09782-x.
8. Anderson K, Peters G (2016) The trouble with negative emissions. Science 354(6309):182-3. doi:10.1126/science.aah4567.
9. Li Y, Chan SH, Sun Q (2015) Heterogeneous catalytic conversion of CO2: a comprehensive theoretical review. Nanoscale 7(19):8663-83. 10.1039/C5NR00092K.
10. Nizio M, Albarazi A, Cavadias S, Amouroux J, Galvez ME, Da Costa P (2016) Hybrid plasma-catalytic methanation of CO2 at low temperature over ceria zirconia supported Ni catalysts. International Journal of Hydrogen Energy 41(27):11584-92. https://doi.org/10.1016/j.ijhydene.2016.02.020.
11. Jean-Luc D, Kazuhiro S, Hironori A (1992) CO2 Hydrogenation over Carbide Catalysts. Chemistry Letters 21(1):5-8. 10.1246/cl.1992.5.
12. Ma J, Sun N, Zhang X, Zhao N, Xiao F, Wei W, et al. (2009) A short review of catalysis for CO2 conversion. Catalysis Today 148(3):221-31. https://doi.org/10.1016/j.cattod.2009.08.015.
13. Sarabadani Tafreshi S, Panahi SFKS, Taghizade N, Jamaati M, Ranjbar M, de Leeuw NH (2022) Thermodynamic and Kinetic Study of Carbon Dioxide Hydrogenation on the Metal-Terminated Tantalum-Carbide (111) Surface: A DFT Calculation. Catalysts 12(10):1275
14. Sarabadani Tafreshi S, Ranjbar M, Jamaati M, Panahi SFKS, Taghizade N, Torkashvand M, et al. (2023) Carbon dioxide hydrogenation over the carbon-terminated niobium carbide (111) surface: a density functional theory study. Physical Chemistry Chemical Physics. 10.1039/D2CP04749G.
15. Sarabadani Tafreshi S, Ranjbar M, Taghizade N, Panahi SFKS, Jamaati M, de Leeuw NH (2022) A first-principles study of CO2 hydrogenation on Niobium-terminated NbC (111) surface. ChemPhysChem 23:e202100781. https://doi.org/10.1002/cphc.202100781.
16. Bratt D. Catalytic CO2 Hydrogenation - Literature Review: Technology Development since 2014. 2016.
17. Li L, Zhao N, Wei W, Sun Y (2013) A review of research progress on CO2 capture, storage, and utilization in Chinese Academy of Sciences. Fuel 108:112-30. https://doi.org/10.1016/j.fuel.2011.08.022.
18. Iandelli A, Palenzona A (1972) Magnetic susceptibility and expansion coefficient of the intermetallic compounds YbAl2 and YbAl3. Journal of the Less Common Metals 29(3):293-7. https://doi.org/10.1016/0022-5088(72)90117-8.
19. McKenna PM (1936) Tantalum Carbide its Relation to other Hard Refractory Compounds. Industrial & Engineering Chemistry 28(7):767-72. 10.1021/ie50319a004.

20. Nino A, Hirabara T, Sugiyama S, Taimatsu H (2015) Preparation and characterization of tantalum carbide (TaC) ceramics. International Journal of Refractory Metals and Hard Materials 52:203-8. https://doi.org/10.1016/j.ijrmhm.2015.06.015.
21. Rowcliffe DJ, Warren WJ (1970) Structure and properties of tantalum carbide crystals. Journal of Materials Science 5(4):345-50. 10.1007/PL00020109.
22. López-de-la-Torre L, Winkler B, Schreuer J, Knorr K, Avalos-Borja M (2005) Elastic properties of tantalum carbide (TaC). Solid State Communications 134(4):245-50. https://doi.org/10.1016/j.ssc.2005.01.036.
23. Viñes F, Sousa C, Liu P, Rodriguez J, Illas F (2005) A systematic density functional theory study of the electronic structure of bulk and (001) surface of transition-metals carbides. The Journal of chemical physics 122(17):174709
24. Kitchin JR, Nørskov JK, Barteau MA, Chen JG (2005) Trends in the chemical properties of early transition metal carbide surfaces: a density functional study. Catalysis Today 105(1):66-73
25. Hugosson HW, Eriksson O, Jansson U, Ruban AV, Souvatzis P, Abrikosov I (2004) Surface energies and work functions of the transition metal carbides. Surface science 557(1-3):243-54
26. Sharma BI, Maibam J, Paul R, Thapa R, Singh RB (2010) Studies on energy band structure of NbC and NbN using DFT. Indian Journal of Physics 84(6):671-4
27. Rodriguez JA, Evans J, Feria L, Vidal AB, Liu P, Nakamura K, et al. (2013) CO2 hydrogenation on Au/TiC, Cu/TiC, and Ni/TiC catalysts: Production of CO, methanol, and methane. Journal of catalysis 307:162-9
28. Quesne MG, Roldan A, de Leeuw NH, Catlow CRA (2018) Bulk and surface properties of metal carbides: implications for catalysis. Physical Chemistry Chemical Physics 20(10):6905-16
29. Levy RB, Boudart M (1973) Platinum-Like Behavior of Tungsten Carbide in Surface Catalysis. Science 181(4099):547-9. 10.1126/science.181.4099.547.
30. Morales-García Á, Calle-Vallejo F, Illas F (2020) MXenes: New Horizons in Catalysis. ACS Catalysis 10(22):13487-503. 10.1021/acscatal.0c03106.
31. Gao G, O'Mullane AP, Du A (2017) 2D MXenes: A New Family of Promising Catalysts for the Hydrogen Evolution Reaction. ACS Catalysis 7(1):494-500. 10.1021/acscatal.6b02754.
32. Wu H, Almalki M, Xu X, Lei Y, Ming F, Mallick A, et al. (2019) MXene Derived Metal–Organic Frameworks. Journal of the American Chemical Society 141(51):20037-42. 10.1021/jacs.9b11446.
33. Liu X, Kunkel C, Ramírez de la Piscina P, Homs N, Viñes F, Illas F (2017) Effective and Highly Selective CO Generation from CO2 Using a Polycrystalline α-Mo2C Catalyst. ACS Catalysis 7(7):4323-35. 10.1021/acscatal.7b00735.
34. Posada-Pérez S, Ramírez PJ, Gutiérrez RA, Stacchiola DJ, Viñes F, Liu P, et al. (2016) The conversion of CO 2 to methanol on orthorhombic β-Mo 2 C and Cu/β-Mo 2 C catalysts: mechanism for admetal induced change in the selectivity and activity. Catalysis Science & Technology 6(18):6766-77
35. Quesne MG, Roldan A, de Leeuw NH, Catlow CRA (2019) Carbon dioxide and water co-adsorption on the low-index surfaces of TiC, VC, ZrC and NbC: a DFT study. Physical Chemistry Chemical Physics 21(20):10750-60
36. Posada-Pérez S, Ramírez PJ, Evans J, Viñes F, Liu P, Illas F, et al. (2016) Highly active Au/δ-MoC and Cu/δ-MoC catalysts for the conversion of CO2: the metal/C ratio as a key factor defining activity, selectivity, and stability. Journal of the American Chemical Society 138(26):8269-78
37. Kunkel C, Vines F, Illas F (2016) Transition metal carbides as novel materials for CO 2 capture, storage, and activation. Energy & Environmental Science 9(1):141-4
38. Silveri F, Quesne MG, Roldan A, De Leeuw NH, Catlow CRA (2019) Hydrogen adsorption on transition metal carbides: a DFT study. Physical Chemistry Chemical Physics 21(10):5335-43
39. Posada-Pérez S, Viñes F, Ramirez PJ, Vidal AB, Rodriguez JA, Illas F (2014) The bending machine: CO2 activation and hydrogenation on δ-MoC(001) and β-Mo2C(001) surfaces. Physical Chemistry Chemical Physics 16(28):14912-21. 10.1039/C4CP01943A.

40. Porosoff MD, Kattel S, Li W, Liu P, Chen JG (2015) Identifying trends and descriptors for selective CO 2 conversion to CO over transition metal carbides. Chemical Communications 51(32):6988-91
41. Xu W, Ramírez PJ, Stacchiola D, Brito JL, Rodriguez JA (2015) The Carburization of Transition Metal Molybdates (MxMoO4, M = Cu, Ni or Co) and the Generation of Highly Active Metal/Carbide Catalysts for CO2 Hydrogenation. Catalysis Letters 145(7):1365-73. 10.1007/s10562-015-1540-5.
42. Li N, Chen X, Ong W-J, MacFarlane DR, Zhao X, Cheetham AK, et al. (2017) Understanding of Electrochemical Mechanisms for CO2 Capture and Conversion into Hydrocarbon Fuels in Transition-Metal Carbides (MXenes). ACS Nano 11(11):10825-33. 10.1021/acsnano.7b03738.
43. Shi Z, Yang H, Gao P, Chen X, Liu H, Zhong L, et al. (2018) Effect of alkali metals on the performance of CoCu/TiO2 catalysts for CO2 hydrogenation to long-chain hydrocarbons. Chinese Journal of Catalysis 39(8):1294-302. https://doi.org/10.1016/S1872-2067(18)63086-4.
44. Tafreshi SS, Moshfegh AZ, de Leeuw NH (2019) Mechanism of Photocatalytic Reduction of CO2 by Ag3PO4(111)/g-C3N4 Nanocomposite: A First-Principles Study. The Journal of Physical Chemistry C 123(36):22191-201. 10.1021/acs.jpcc.9b04493.
45. Ou Z, Qin C, Niu J, Zhang L, Ran J (2019) A comprehensive DFT study of CO2 catalytic conversion by H2 over Pt-doped Ni catalysts. International Journal of Hydrogen Energy 44(2):819-34. https://doi.org/10.1016/j.ijhydene.2018.11.008.
46. Morales-García Á, Fernández-Fernández A, Viñes F, Illas F (2018) CO2 abatement using two-dimensional MXene carbides. Journal of Materials Chemistry A 6(8):3381-5. 10.1039/C7TA11379J.
47. Morales-García Á, Mayans-Llorach M, Viñes F, Illas F (2019) Thickness biased capture of CO2 on carbide MXenes. Physical Chemistry Chemical Physics 21(41):23136-42. 10.1039/C9CP04833B.
48. Edamoto K, Yamazaki M, Noda T, Ozawa K, Otani S (2001) Hydrogen adsorption on a HfC(111) surface: angle-resolved photoemission study. Journal of Electron Spectroscopy and Related Phenomena 114-116:495-9. https://doi.org/10.1016/S0368-2048(00)00249-8.
49. Aizawa T, Hayami W, Souda R, Otani S, Ishizawa Y (1997) Hydrogen adsorption on transition-metal carbide (111) surfaces. Surface Science 381(2):157-64. https://doi.org/10.1016/S0039-6028(97)00108-8.
50. Tokumitsu S, Anazawa T, Tanabe A, Sekine R, Miyazaki E, Edamoto K, et al. (1996) Interaction of hydrogen with ZrC(111) surface: angle-resolved photoemission study. Surface Science 351(1):165-71. https://doi.org/10.1016/0039-6028(95)01274-5.
51. von Roedern B, Moddel G (1980) Gap states in hydrogenated amorphous silicon: A comparison of photoemission and photoconductivity results. Solid State Communications 35(6):467-71. https://doi.org/10.1016/0038-1098(80)90250-1.
52. Kitchin JR. Tuning the electronic and chemical properties of metals : bimetallics and transition metal carbides,PhD Thesis, Dept of Materials Science and Engineering: University of Delaware; 2004. p. 196.
53. Gilles R, Mukherji D, Karge L, Strunz P, Beran P, Barbier B, et al. (2016) Stability of TaC precipitates in a Co-Re-based alloy being developed for ultra-high-temperature applications. Journal of Applied Crystallography 49(4):1253-65. 10.1107/S1600576716009006.
54. Hocker S, Lipp H, Schmauder S, Bakulin AV, Kulkova SE (2021) Ab initio investigation of Co/TaC interfaces. Journal of Alloys and Compounds 853:156944. https://doi.org/10.1016/j.jallcom.2020.156944.
55. Choi Y, Liu P (2009) Mechanism of Ethanol Synthesis from Syngas on Rh(111). Journal of the American Chemical Society 131(36):13054-61. 10.1021/ja903013x.
56. Dzade NY, de Leeuw NH (2021) Activating the FeS (001) Surface for CO2 Adsorption and Reduction through the Formation of Sulfur Vacancies: A DFT-D3 Study. Catalysts 11(1):127
57. Tominaga H, Nagai M (2005) Density functional study of carbon dioxide hydrogenation on molybdenum carbide and metal. Applied Catalysis A: General 282(1):5-13. https://doi.org/10.1016/j.apcata.2004.09.041.

58. Sun W, Kuang X, Liang H, Xia X, Zhang Z, Lu C, et al. (2020) Mechanical properties of tantalum carbide from high-pressure/high-temperature synthesis and first-principles calculations. Physical Chemistry Chemical Physics 22(9):5018-23. 10.1039/C9CP06819H.
59. Kresse G, Joubert D (1999) From ultrasoft pseudopotentials to the projector augmented-wave method. Physical Review B 59(3):1758-75. 10.1103/PhysRevB.59.1758.
60. Perdew JP, Burke K, Ernzerhof M (1998) Perdew, Burke, and Ernzerhof Reply. Physical Review Letters 80(4):891-. 10.1103/PhysRevLett.80.891.
61. Grimme S (2011) Density functional theory with London dispersion corrections. WIREs Computational Molecular Science 1(2):211-28. https://doi.org/10.1002/wcms.30.
62. https://icsd.products.fiz-karlsruhe.de/.
63. Qi K-Z, Wang G-C, Zheng W-J (2013) A first-principles study of CO hydrogenation into methane on molybdenum carbides catalysts. Surface Science 614:53-63. https://doi.org/10.1016/j.susc.2013.04.001.
64. Liu P, Rodriguez JA (2006) Water-gas-shift reaction on molybdenum carbide surfaces: essential role of the oxycarbide. J Phys Chem B 110(39):19418-25. 10.1021/jp0621629.
65. Porosoff MD, Yang X, Boscoboinik JA, Chen JG (2014) Molybdenum Carbide as Alternative Catalysts to Precious Metals for Highly Selective Reduction of CO2 to CO. Angewandte Chemie 126(26):6823-7. doi:10.1002/ange.201404109.